Observation of Retardation Effects in the Spectrum of Two-Dimensional Plasmons

I.V. Kukushkin,[1,2] J. H. Smet,[1] S. A. Mikhailov,[1] D.V. Kulakovskii,[1,2] K. von Klitzing,[1] and W. Wegscheider[3,4]

[1]*Max-Planck-Institut für Festkörperforschung, Heisenbergstrasse 1, D-70569 Stuttgart, Germany*
[2]*Institute of Solid State Physics, Russian Academy of Sciences, Chernogolovka, 142432 Russia*
[3]*Walter Schottky Institut, Technische Universität München, 85748 Garching, Germany*
[4]*Institut für Experimentelle und Angewandte Physik, Universität Regensburg, D-93040 Regensburg, Germany*

(Received 8 January 2003; published 15 April 2003)

Retardation effects, theoretically predicted more than 35 years ago, are observed in the spectrum of two-dimensional plasmons in high-electron-mobility GaAs/AlGaAs quantum wells. In zero magnetic field, a strong reduction of the resonant plasma frequency is observed due to the hybridization of the plasma and light modes. In a perpendicular magnetic field B, hybrid cyclotron-plasmon modes appear with a very unusual dependence of the frequency on B field. Experimental results are in excellent agreement with the theory.

DOI: 10.1103/PhysRevLett.90.156801 PACS numbers: 73.20.Mf, 71.36.+c

Plasma oscillations in two-dimensional electron systems (2DES) were predicted in 1967 [1] and experimentally observed about ten years later in a sheet of electrons on liquid helium [2] and in silicon inversion layers [3,4]. These and numerous subsequent experiments (see review articles [5,6]) quantitatively confirmed the predicted 2D-plasmon dispersion [1,7]

$$\omega_p^2(q) = \frac{2\pi n_s e^2}{m^\star \epsilon(q)} q; \tag{1}$$

n_s and $m^\star$ are the density and the effective mass of 2D electrons, and $\epsilon(q)$ is the effective dielectric permittivity of the surrounding medium. In semiconductor systems (such as Si inversion layers or GaAs/AlGaAs heterostructures), far-infrared transmission spectroscopy was commonly used for detecting these excitations as well as Raman scattering [8]. In the former method, the 2D plasmon wave vector q (typically $\sim 10^4$/cm) was determined by an adjacent metal grating, which served to couple plasmons with the electromagnetic radiation.

The spectrum described by Eq. (1) was derived in the quasielectrostatic approximation. The influence of electrodynamic effects on the dispersion was theoretically addressed in the very first paper by Stern [1], as well as in a number of subsequent publications [9–12]. Retardation effects become essential at $q \simeq 2\pi n_s e^2/m^\star c^2$ and $\omega \simeq 2\pi n_s e^2/m^\star c\sqrt{\epsilon}$, when the phase velocity of the plasmons derived from Eq. (1) approaches the light velocity c. For typical parameters of GaAs/AlGaAs heterostructures ($n_s \simeq 3 \times 10^{11}$ cm^{-2}, $m^\star = 0.067 m_0$, and $\epsilon \simeq 12.8$), this yields $q \simeq 10^{-1}$ cm^{-1} and $\omega/2\pi \simeq 30$ GHz. The observation of 2D plasmons at such low frequencies was not possible in the early eighties, because the momentum relaxation rate imposed a lower bound on the linewidth of plasma resonances and was typically not smaller than 100 GHz. [3–6]. However, during the past two decades the quality of samples has dramatically improved and the mobility μ increased by several orders of magnitude. From theory [10], it is anticipated that in high-electron-mobility samples (quantitatively at $2\pi e n_s \mu/c\sqrt{\epsilon} > 1$, so that for the above-mentioned parameters μ should exceed 0.4×10^6cm^2/Vs) weakly damped 2D plasmon-polaritons [coupled modes of light and the 2D plasmons of Eq. (1)] exist at all frequencies, not only at $\omega\tau \gg 1$. Nevertheless, to the best of our knowledge, such retardation effects in the spectrum of 2D plasmons have remained unexplored in experiment up to this date. In this Letter, we report their first observation.

Several low and high-density ($n_s = 0.4$–6.6×10^{11} cm^{-2}) GaAs/Al_xGa_{1-x}As single quantum well samples with a well width of 25–30 nm and electron mobilities μ between 1–5 $\times 10^6$ cm^2/Vs were investigated. The linewidth of the resonant microwave absorption peaks was very small (1–5 GHz). It allowed to measure the plasmon-cyclotron resonance at rather low microwave frequencies (10–50 GHz). For measurements of the density, we resorted to magnetoluminescence methods [13]. They provide an accuracy better than 0.1% due to the appearance of extremely narrow peaks in the noise spectrum at integer filling factors. In order to study dimensional magnetoplasma modes of electrons, disk-shaped mesas were fabricated with diameters of 0.1, 0.2, 0.3, 0.4, 0.5, 0.6, 1, 2, and 3 mm [14,15]. For optical detection of magnetoplasma resonances, the sensitivity of luminescence spectra to resonant microwave absorption was exploited [16,17]. The technique is based on a comparison between spectra in the absence and presence of microwave radiation. The spectra are recorded with the help of a CCD-camera and a double-grating spectrometer with a spectral resolution of 0.03 meV. A stabilized semiconductor laser with a wavelength of 750 nm supplies cw-photoexcitation at a power level of approximately 0.1 mW distributed across the entire area of the disk. The microwave excitation is produced with a HP-83650B generator, which covers frequencies up to 50 GHz.

The samples were placed in the microwave-electric field maximum inside a 16-mm waveguide, which was short-circuited at one end near the sample. The microwave power at the entrance was 10 μW to 0.2 mW. Other details of our method have been published elsewhere [14,15,17].

In Fig. 1 the B-field dependencies of the magnetoplasma resonance frequencies are plotted for samples with different densities n_s and mesa diameters (to avoid interpretation difficulties due to a variation of the microwave power as a function of the incident microwave frequency, the magnetic field was scanned at fixed microwave frequency instead). Figure 1(a) depicts results for two samples with relatively low density $n_s = 0.42 \times 10^{11}$ cm^{-2} and small diameters of $d = 0.1$ and 0.2 mm. The measured spectra show the typical double mode behavior that has been observed on many occasions in quantum dots and classical disks (e.g., [18–21]). Both modes are well understood theoretically [18,19,22–25]. The upper bulk-magnetoplasmon mode approaches the cyclotron resonance (dashed lines) but never crosses it. The lower edge magnetoplasmon mode tends to zero with increasing magnetic field. Both modes start off at $B = 0$ from the same frequency. It deviates slightly (about 10%) from the frequency $\omega_0 = (2\pi n_s e^2/m^\star R\bar{\epsilon})^{1/2}$(marked by arrows) predicted with Eq. (1) when substituting $q = 1/R$; here $\bar{\epsilon} = (1 + \epsilon)/2$ is the average dielectric constant of free space and GaAs and R is the disk radius.

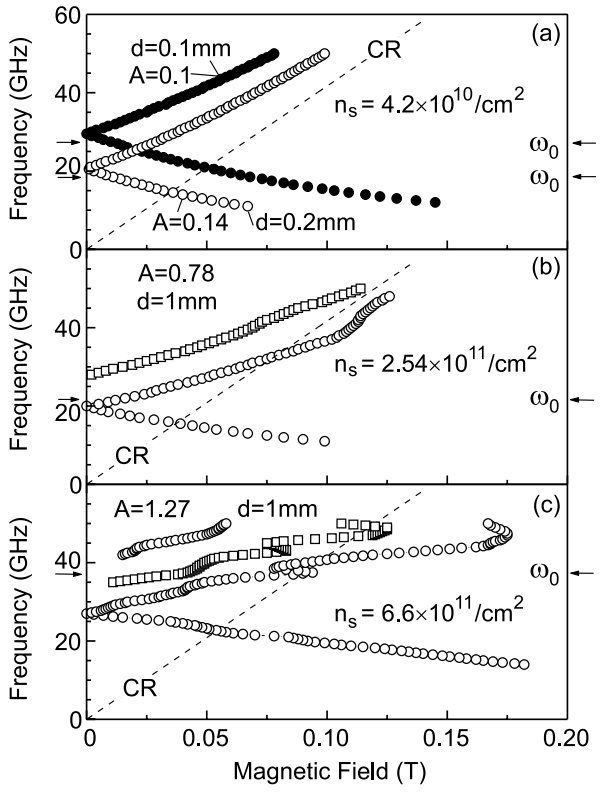

FIG. 1. 2D magnetoplasmon spectra at 1.5 K for several samples with various electron densities and different mesa diameters. The retardation parameter A has also been included.

The situation drastically alters in samples with higher electron density and larger diameter. Figure 1(b) shows results for a sample with $n_s = 2.54 \times 10^{11}$ cm^{-2} and $d = 1$ mm. A number of new features emerges: (i) at $B = 0$ the resonant plasma frequency is markedly smaller than ω_0, (ii) the upper bulk magnetoplasma mode intersects the cyclotron resonance line at a certain finite value of the B field, (iii) the slope $(df_\pm/dB)_{B\to 0}$ is considerably smaller than the conventional result $|d\omega_\pm/d\omega_c| = 1/2$ [18] (in Fig. 1(a) the slope $d\omega/d\omega_c$ is close to 0.5; ω_c is the cyclotron frequency). After crossing the cyclotron resonance the linewidth of the bulk-magnetoplasmon mode starts to increase. Also, a second high-frequency plasma mode appears in the spectrum. A further increase of the electron density and/or mesa diameter leads to an even stronger manifestation of these features, as illustrated in Fig. 1(c). It displays the spectra for a sample with $n_s = 6.6 \times 10^{11}$ cm^{-2} and $d = 1$ mm. The B-field dependence of the bulk magnetoplasma modes exhibits intriguing zigzag shaped behavior at higher frequencies. Even a third high-frequency bulk magnetoplasma mode is detected.

A simple qualitative analysis already suggests retardation effects as the origin of these phenomena. The dimensionless parameter A defined as the ratio of the plasma frequency to the frequency of light with the same wave vector $q = 1/R$, $A = \omega_0 \epsilon^{1/2} R/c$, may serve as an indicator for the importance of retardation. This parameter grows with both n_s and R according to $A \propto (n_s R)^{1/2}$, and in all previous experimental studies never exceeded 0.1–0.15. For the two samples, shown in Fig. 1(a), A takes on the value 0.1 and 0.14 for $d = 0.1$ and $d = 0.2$ mm, respectively, so that no influence of the finite light velocity on the measured spectra is expected. For the samples of Fig. 1(b) and 1(c) instead, A equals 0.78 and 1.27, so that it is plausible to relate the observed phenomena with the influence of retardation. To support this assertion, calculations of resonant magnetoplasma modes in a disk-shaped sample including retardation were performed. Using a slightly modified approach in comparison with Ref. [23], a full system of Maxwell equations was solved to extract the B-field dependence of the magnetoplasma modes in a disk with density profile $n_s(r) = n_s\theta(R - r)$, where θ is the Heaviside step function. The eigenmodes are characterized by angular momentum L and the radial quantum number n (see [19,23,26–28]). Only the lowest $n = 1$ modes with $L = 1, 2$, and 3 are plotted in Fig. 2 for values of A relevant to our experiment. The overall agreement between theory and experiment is evident. A detailed quantitative comparison of the measured and calculated frequencies allows to identify the higher bulk-magnetoplasmon modes for $A = 0.78$ and $A = 1.27$ as the modes with higher angular momenta $L = 2$ and 3 and with the lowest value of $n = 1$ ($n > 1$ modes have larger frequency).

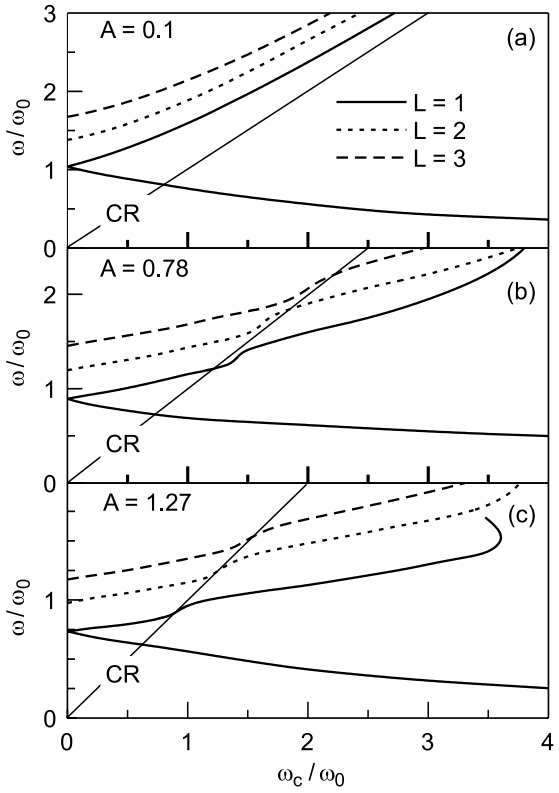

FIG. 2. Calculated dependence of the normalized magnetoplasma resonances ω/ω_0 versus ω_c/ω_0, i.e., normalized magnetic field, for a disk-shaped sample. Only the lowest $n = 1$ modes with angular momenta $L = 1, 2, 3$ are shown. The edge magnetoplasmon modes with negative B dispersion are not shown for $L = 2$ and 3. [In Fig. 1(a) the two pairs of $\omega_\pm$ are the $n = L = 1$ modes for two different samples, not the modes with $L > 1$.]

A detailed discussion of experimental and theoretical spectra across the whole range of B fields will be postponed to a more comprehensive publication. Here, we focus on a quantitative analysis at small fields $B \to 0$. In Fig. 3(a) the dependence of $\omega_{B=0}/\omega_0$ on parameter A is presented for seven samples with different n_s and R. $\omega_{B=0}/\omega_0$ starts from 1.1 at small A and drops down to 0.5 as A increases up to 2.2. The solid curve is the corresponding calculated dependence. At $A = 0$ our result coincides with that calculated by Fetter in the quasistatic approximation [23]. The theory agrees well with the experiment and the disagreement of only a few percent may be due to an uncertainty in the effective dielectric constant of the surrounding medium $\bar{\epsilon}$, which in the real system may depend on the sample size, the presence of a waveguide, etc. In Fig. 3(b) the dependence of the slope $|d\omega_\pm/d\omega_c|$ on A as $B \to 0$ is plotted. This slope is even more sensitive to A—it drops by a factor of 4 when A increases up to 2.2. The theoretical solid curve has also been included and agrees well with experiment.

Finally, the data are analyzed to quantitatively verify the 2D plasmon dispersion $\omega(q)$ predicted in Ref. [1]. When taking into account retardation effects, Stern de-

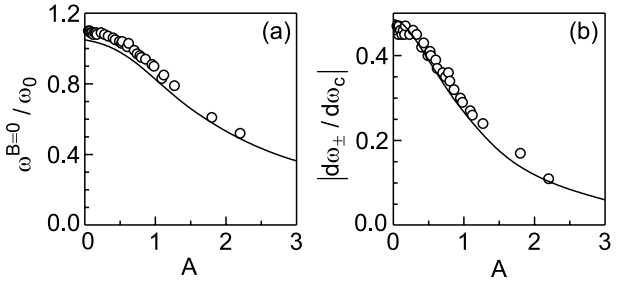

FIG. 3. (a) Normalized resonance frequency at $B = 0$ $\omega_{B=0}/\omega_0$ and (b) their slope $|d\omega_\pm/d\omega_c|$ as $B \to 0$ vs the retardation parameter $A = \omega_0\sqrt{\epsilon}R/c$; $\omega_0 = (2\pi n_s e^2/m^\star\bar{\epsilon}R)^{1/2}$. Symbols are experimental points; solid curves correspond to theory.

rived that the 2D-plasmon dispersion may be written as

$$q^2 = \epsilon\omega^2/c^2 + \left(\frac{\omega^2}{2\pi n_s e^2/m^\star\bar{\epsilon}}\right)^2. \quad (2)$$

According to this expression, the data should fall onto straight lines for all densities, frequencies, and mesa diameters, when they are presented with ω^2 as the abscissa and q^2/ω^2 as the ordinate. In Fig. 4(a) the experimental results are plotted as a function of $1/(f^2d^2)$ with f^2 as the ordinate to allow for an immediate comparison with the functional dependence predicted by this equation. The data indeed confirm it. The intersections of the lines with the axes define two important points. On the vertical axis the intersection yields the radiative decay rate Γ in an infinite sample [25]:

$$\Gamma^2 = (2\pi n_s e^2\epsilon^{1/2}/m^\star c\bar{\epsilon})^2. \quad (3)$$

It depends only on the electron density and not on the mesa diameter. Since other parameters in Eq. (3) are well known, the electron density can be extracted from the measured value of Γ and compared with the density obtained from oscillations observed in magnetoluminescence spectra [13] to check for consistency. The values indeed agree very well. Another important feature in Fig. 4(a) is the common crossing point of all lines at $f = 0$ and $(fd)^{-2} = 9.6 \times 10^{-16}$ c^2/m^2. According to Eq. (2) this value should correspond to $q^2/\omega^2 = \epsilon/c^2 = 1.43 \times 10^{-16}$ c^2/m^2. It allows one to deduce a relationship between the wave vector q and the diameter d of the disk-shaped mesa. One finds that $q = 2\alpha/d$ where $\alpha \approx 1.2$. In the literature, there still exist discrepancies in the numerical value of this parameter among theories as well as experiments. Theoretically, this coefficient depends on the electron density profile near the edge of the disk and was found to be ≈ 1.05 for a sharp [23] and $3\pi/8 \approx 1.18$ for a smooth semielliptic density profile [22].

The knowledge of the relationship between wave vector and disk diameter ($q = 2.4/d$) puts us in a position to determine the dispersion of the zero field plasmon mode by plotting the dependence of the resonance frequency as a function of the inverse of the mesa diameter. This

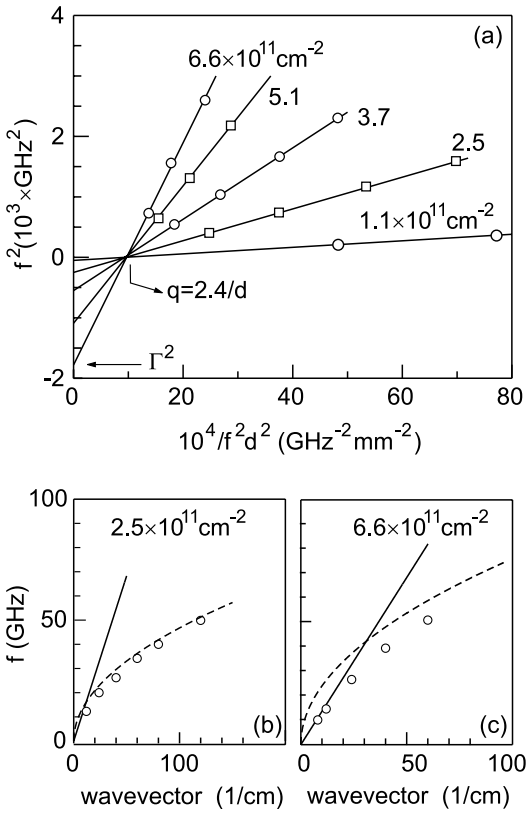

FIG. 4. (a) Experimental data plotted on appropriate axes to determine the characteristic frequency Γ and the relation between the wave vector q and the disk diameter d, $qd = 2.4$, as outlined in the text. (b),(c) The 2D-plasmon-polariton dispersion deduced from experiments for two samples with different density. Symbols are experimental points. Curves are the dispersion of light (solid) and the 2D plasmon dispersion calculated in the quasistatic approximation [Eq. (1)].

exercise has been carried out in Figs. 4(b) and 4(c) for two different densities $n_s = 2.5 \times 10^{11}$ and 6.6×10^{11} cm^{-2}. For the sake of comparison, the dispersion of light $\omega = 2\pi f = cq/\sqrt{\epsilon}$ (solid curve) and of the 2D-plasmon mode described by Eq. (1) $\omega = f/2\pi = (2\pi n_s e^2 q/m^\star \bar{\epsilon})^{1/2}$ (dashed curve) have been included. At small concentrations the dispersion corresponds mainly to the pure 2D-plasmon law, whereas for the highest concentration coupling between the plasma mode and light takes place in accordance with Ref. [1].

In summary, the 2D-magnetoplasmon excitation spectra in the small-wave vector and low-frequency regimes, where an influence of retardation is expected, have been studied. Clear signatures for retardation effects were identified. Especially at finite perpendicular B fields, anomalous hybrid magnetoplasmon-cyclotron modes with a very unusual field dependence of the resonance frequency have been uncovered. Experimental results were compared with theoretical predictions of [1] for 2D-plasmon-polaritons in an infinite 2DES at $B = 0$ as well as for a disk-shaped sample in zero and finite magnetic fields. These calculations accurately reproduce the experimental data.

Financial support through the Max-Planck and Humboldt Research Awards and from the Russian Fund of Fundamental Research, the German Science Foundation and the German Ministry of Science and Education is gratefully acknowledged. We thank K. Eberl for the high-density sample.

[1] F. Stern, Phys. Rev. Lett. **18**, 546 (1967).
[2] C. C. Grimes and G. Adams, Phys. Rev. Lett. **36**, 145 (1976).
[3] S. J. Allen, Jr., D. C. Tsui, and R. A. Logan, Phys. Rev. Lett. **38**, 980 (1977).
[4] T. N. Theis, J. P. Kotthaus, and P. J. Stiles, Solid State Commun. **26**, 603 (1978).
[5] T. N. Theis, Surf. Sci. **98**, 515 (1980).
[6] D. Heitmann, Surf. Sci. **170**, 332 (1986).
[7] A. V. Chaplik, Zh. Eksp. Teor. Fiz. **62**, 746 (1972) [Sov. Phys. JETP **35**, 395–398 (1972)].
[8] D. Richards, B. Jusserand, H. Peric, and B. Etienne, Phys. Rev. B **47**, 16 028 (1993).
[9] K. W. Chiu and J. J. Quinn, Phys. Rev. B **9**, 4724 (1974).
[10] V. I. Fal'ko and D. E. Khmel'nitskii, Zh. Eksp. Teor. Fiz. **95**, 1988 (1989) [Sov. Phys. JETP **68**, 1150–1152 (1989)].
[11] A. O. Govorov and A. V. Chaplik, Zh. Eksp. Teor. Fiz. **95**, 1976 (1989) [Sov. Phys. JETP **68**, 1143–1144 (1989)].
[12] S. A. Mikhailov, Pis'ma Zh. Eksp. Teor. Fiz. **57**, 570 (1993) [JETP Lett. **57**, 586–590 (1993)].
[13] O. V. Volkov *et al.*, JETP Lett. **71**, 383 (2000) [Pis'ma Zh. Eksp. Teor. Fiz. **71**, 558 (2000)].
[14] S. I. Gubarev *et al.*, JETP Lett. **72**, 324 (2000) [Pis'ma Zh. Eksp. Teor. Fiz. **72**, 469 (2000)].
[15] M. Y. Akimov *et al.*, JETP Lett. **72**, 460 (2000) [Pis'ma Zh. Eksp. Teor. Fiz. **72**, 662 (2000)].
[16] B. M. Ashkinadze and V. I. Yudson, Phys. Rev. Lett. **83**, 812 (1999).
[17] I. V. Kukushkin, J. H. Smet, K. von Klitzing, and W. Wegscheider, Nature (London) **415**, 409 (2002).
[18] S. J. Allen, Jr., H. L. Störmer, and J. C. M. Hwang, Phys. Rev. B **28**, 4875 (1983).
[19] D. C. Glattli *et al.*, Phys. Rev. Lett. **54**, 1710 (1985).
[20] T. Demel, D. Heitmann, P. Grambow, and K. Ploog, Phys. Rev. Lett. **64**, 788 (1990).
[21] W. Hansen, J. P. Kotthaus, and U. Merkt, in *Semiconductors and Semimetals*, edited by M. Read (Academic Press, New York, 1992), Vol. 35, p. 279.
[22] R. P. Leavitt and J. W. Little, Phys. Rev. B **34**, 2450 (1986).
[23] A. L. Fetter, Phys. Rev. B **33**, 5221 (1986).
[24] V. A. Volkov and S. A. Mikhailov, Zh. Eksp. Teor. Fiz. **94**, 217 (1988) [Sov. Phys. JETP **67**, 1639–1653 (1988)].
[25] S. A. Mikhailov, Phys. Rev. B **54**, 10 335 (1996).
[26] S. S. Nazin and V. B. Shikin, Fiz. Nizk. Temp. **15**, 227 (1989) [Sov. J. Low Temp. Phys. **15**, 127–131 (1989)].
[27] V. Shikin, S. Nazin, D. Heitmann, and T. Demel, Phys. Rev. B **43**, 11 903 (1991).
[28] Z. L. Ye and E. Zaremba, Phys. Rev. B **50**, 17217 (1994).